Mode Analysis of Self-Pulsations of PDR Lasers

A Supplement to the Radziunas-Report [1]

H.-J. Wünsche *

16.11.1999

1 Introduction

Mindaugas Radziunas has supplemented his TWE-modelling of the SP-dynamics with a mode calculation tool. On this base he described in [1] how the modes change during a SP or when the phase current is varied. This gave a much deeper insight in what happens in these selfpulsating lasers.

Parallel to and independent of him, I have build up during the last months another type of mode calculation connected with a single mode stability analysis.

This paper presents the basic idea of my approach and gives a comparison with that of Mindaugas for the examples in [1]. The device is sketched in Fig. 1. I have to mention a comparison with calculations of Jan Sieber done in May/June that allowed already to remove some bugs from my program. Now, Jan Sieber's and my program give the same mode parameters – at least for the compared examples. So there is good hope to get coincidence also with Mindaugas results.

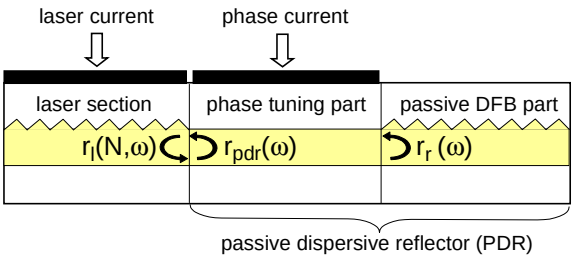

Fig. 1:
Schema of a PDR laser. Only the carriers in the gain section couple to the optical field. The waveguide in all PDR subsections is passive. It consists of a phase tuning part without grating and an additional dispersive reflector, here a passive DFB section.

2 The basic idea of my PDR-approach

PDR means passive dispersive reflector. I consider devices with only one active laser section. This laser section is supplemented by an arbitrary passive dispersive reflector. Our standard device with two DFB sections and an integrated phase tuning section is of this type as long as the reflector DFB is pumped just at transparency. I regard a spatially constant carrier density N in the active section. The situation refered to in the following is as sketched in Fig. 1.

A mode in the sense of this paper belongs to a fixed density. It is an optical field that for this given density propagates without changing its spatial shape. The field of a mode depents on time by an exponential factor $\exp(i\omega t)$ that is unique for all field components and all positions. The mode frequency ω is in general complex. Its real part is synonymous to the wavelength according to $\lambda = 2\pi c/\Re e\,\omega$. The imaginary part determines the evolution of the mode field intensity. It decays exponentially for a positive one, explodes exponentially for a negative sign and remains constant only for $\Im m\,\omega = 0$. Modes with $\Im m\,\omega = 0$ are called 'stationary' or 'at

*Humboldt-Universität zu Berlin,Institut für Physik, Invalidenstr. 110, D-10115 Berlin, Germany (Email: ede@physik.hu-berlin.de)

threshold'. Accordingly, the density at which a given mode is at threshold is its threshold density. Different modes have different threshold densities.

In a stationary laser state neither the optical intensity nor the carrier density vary with time. This requires

- only one mode operates – otherwise beating caused a nonstationary intensity,
- this lasing mode is at threshold – otherwise it would decay or explode,
- and the $\Im m\,\omega$ of all other modes is positive – otherwise they would explode.

For any nonstationary state, especially during a self-pulsation, N varies with time t. Modes seem to make no sense in this case. However, the optical field can be regarded as composed of the fields of a series of modes. Those mode contributions with a temporary negative $\Im m\,\omega$ will tend to raise and can become dominant for a certain time. Therefore, it is important to determine the mode properties also for nonstationary situations.

Generally, the mode frequencies of a PDR laser solve the equation

$$r_l(N,\omega)\; r_{pdr}(\omega) = 1 \tag{1}$$

Here r_{pdr}, r_l denote the amplitude reflectivities of the PDR and of the laser section, respectively. This equation is obvious: r_{pdr} is per definition the amplitude coming back from the reflector divided by the amplitude traveling into the reflector and r_l is the reverse. This equation is highly nonlinear and has an infinite set of solutions ω_m labeled by the mode index m. The calculation of all relevant modes requires often a cumbersome iteration procedure. The approach to be presented avoids these iterations to a large extend.

It is easy to calculate the reflectivities r_l, r_{pdr} from the travelling wave equations (TWE). The time derivative becomes a simple multiplication with the frequency, $\partial_t \cdots \to i\omega \cdots$. This transforms the partial TWE into the ordinary coupled mode equations (CME). The CME are first order in the space coordinate z. For calculating r_{pdr}, one starts with an outgoing wave on the outer facet of the PDR and integrates the CME inwards to the facet at the border to the laser section. The quotient of the forward and backward amplitudes obtained there gives r_{pdr}. The same is done from the left for r_l. These calculations are straightforward. No iteration is required.

In the next step we take profit from our knowledge on the phase tuning section. It holds

$$r_{pdr}(\omega) = e^{-2i\beta_p(\omega)L_p} r_r(\omega), \tag{2}$$

where β_p is the complex propagation constant of the wave guide of the phase section and L_p its length. r_r denotes the reflectivity of the PDR without phase tuning section (the reflectivity of the DFB reflector in our case). Operating close to a central frequency ω_0, we have $\beta_p(\omega) \approx \beta_p(\omega_0) + \Omega/v_g$ with the relative frequency $\Omega = \omega - \omega_0$. Inserting this and shifting all frequency dependent parts to the left hand side, Equ. (1) becomes

$$r_l(N,\Omega)\; r_r(\Omega)\; e^{i\Omega T} = e^{-i\varphi}\; e^{-d}. \tag{3}$$

Here some new notations have been introduced. $T = 2L_p/v_g$ is the round trip time of the phase section. It is responsible for its contribution to the dispersion. $\varphi = 2\Re e\,\beta_p(\omega_0)L_p$ is the static phase shift that can be tuned by changing the phase current. $d = \alpha_p L_p$ is the damping of the wave due to the absorption in the phase section.

Equ. (3) is basic. It can be interpreted and used in different manners. The usual point of view is to fix all parameters, including φ and d, and to search a solution. Then this complex equation is equivalent to two real equations for the 3 real variables $N, \Re e\,\Omega, \Im m\,\Omega$. This defines some curved lines in the 3D space spanned by these variables. The calculation of these lines requires iterations.

When studying the properties of the PDR lasers, the point of view is often a bit different. It is well known that the phase φ plays an important role and allows, e.g., to switch on and of the SP. Therefore, it is not sufficient to calculate the modes only for one given phase. One needs their dependency on the phase over the whole period. A similar point of view is useful with respect to the damping: When tailoring a PDR for a specific application, we have to know how the modes depend on d. Allowing for arbitrary φ and d, Equ. (3) represents no restriction for N, Ω. This suggests to regard the inverse problem, i.e., to vary N, Ω and to calculate φ, d. This is simple. The analytic solution is

$$i\varphi(N,\Omega) + d(N,\Omega) = \ln\left(r_l(N,\Omega)\; r_r(\Omega)\; e^{i\Omega T}\right). \tag{4}$$

Using the data calculated from this formula, I can can construct some interesting types of drawings without iterations. These will be discussed in the following.

2.1 Stationary Modes: density-wavelength-plot

Remember that a mode with $\Im m\,\Omega = 0$ is called stationary or at its threshold. Supposing this; I calculate phase and damping according to (4) by varying $\lambda = 2\pi c/\Re e\,\Omega$ and N over a rectangular grid. With Origin, I plot lines of constant damping and lines of constant phase from these data matrices. The intersections of a line with a given d and a line with a given φ give the threshold densities and wavelengths of all modes for these parameters within the scanned N, λ-domain.

Example: single section DFB laser

One example makes the things more clear than thousand words. I regard the following special case of the device of Fig. 1: the right facet is reflection coated (reflectivity 1), the length of the passive DFB-part is zero, the phase tuning section is necligibly short. This corresponds to a single section DFB laser with an antireflection coated left facet and a right facet with a power reflectivity $R = \exp(-2d)$. So the following parametervalues $d = 0, 1, 2, \infty$ correspond to the reflectivities $R = 1, 0.37, 0.14, 0$.

The density-wavelength plot of such a device is drawn in Fig. 2. Note that not the absolute wavelength is used as abscissa. Instead, the wavelength relative to the center of the laser stop band

$$\lambda_{rel}(N) = \lambda(N) - \frac{\alpha_H \Gamma g' \lambda_0^2}{4\pi n_g}(N - N_{tr}) \tag{5}$$

is used here and will be used in all following figures . Without this transformation the main axis of the ellipses had a strong negative slope resulting in a less clear picture.

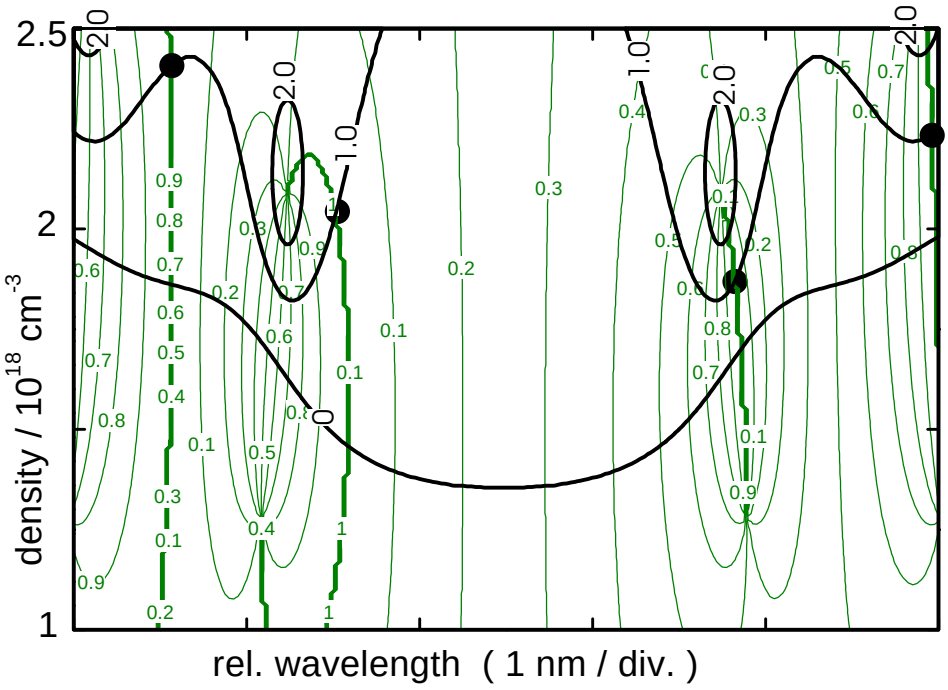

Fig. :
Stationary modes of a single section DFB laser in the density-wavelength-plane. The left facet is antireflection coated. The right facet has a finite amplitude reflectivity r. The labels at the fat lines give the magnitude $d = -\ln(|r|)$ and the labels at the thin lines the phase $\varphi = \arg(r)$ of the reflectivity r.

The dots in the center of the $d = 2$ ellipses indicate the limit $d \to \infty$. They give the threshold density and the threshold wavelengths of the two well known modes of a single section DFB laser without any reflectivity. The region between these two points is the stop band of this laser.

The case $d = 2$ corresponds to the small reflectivity $R = 0.14$. This small feedback causes only a small change of the threshold densities of the two modes. Whether the threshold goes up or down depends on the phase of the reflectivity. When the phase is increased by one period, the modes travel counterclockwise along small ellipses centered at the modes of the feedback free device.

Not only the main modes produce such ellipses but also all side modes, however, at higher densities. The lower part of the second side lobe is observable in the right upper part of the figure. Notice that the electronic blueshift brings the wavelengths of the long wave ellipses closer together whereas they are stretched on the short wave side of the stop band. This makes the two sides of the stop band inequivalent in case of longitudinal hole burning, when the density varies along the laser axis.

Although the shapes of the ellipses on the two sides of the stop band are identical, the phases behave different. E.g., for $\varphi = 0$ the left mode is close to the minimum, whereas the right mode is noticeably higher. For this phase, the left mode is lasing because it has the lower threshold. For other phases, the situation is reverse. Thus, the phase of the reflectivity decides which mode lases. This is well known.

With further increasing feedback, the diameter of the ellipses grows until the diffent modes merge. In our example, this is already the case for $d = 1$, i.e., for the reflectivity $R = 0.37$ of a cleaved facet. With increasing φ, every mode now travels along this line from left to right. After one period, the mode m arrives on the former position of the mode $m + 1$. Nevertheless, the two sides of the stop band give still the lowest thresholds, in this case.

This changes completely for $d = 0$: now a very low threshold is achieved in the middle of the stop band at $\varphi = 3/4$. This is also a well known case. It corresponds to a reflectivity $R = 1$ with phase $-1/4$ that in turn is equivalent to a laser with the double length and a quarter wave phase jump in the middle. Such $\lambda/4$-laser are well known to oscillate in the middle of the stop band at a low theshold.

Concluding this subsection: the described density-wavelength plot is not only easy to obtain but gives a nice overview over the mode properties of the PDR-laser.

2.2 Which mode is the lasing mode: $\Im m\,\Omega$-wavelength-plot

The density-wavelength plot discussed before gives all stationary modes within a given domain. For $d = 1, \varphi = 0$, e.g., Fig. exhibits 4 different modes (fat black dots). Note that all they belong to different carrier densities. Now we ask, which of them is the lasing mode. This requires for every of these dots to check whether $\Im m\,\Omega > 0$ for all other modes at the same carrier density. For these purposes, we fix N to one of the dots, vary vary the real and imaginary parts of Ω and plot again the lines of constant d and φ. This procedure is repeated for all dots.

Example: single section DFB laser

First we fix $N = 1.87 \times 10^{18}\mathrm{cm}^{-3}$ to the lowest dot. Fig. gives the overview over the modes for this density. Now, the black dots represent the modes for $d = 1, \varphi = 0$ at this density. All dots are above zero but the lowest one that has $\Im m\,\Omega = 0$. Hence, this lowest dot is the lasing mode. It represents the same state as the lowest dot in Fig. .

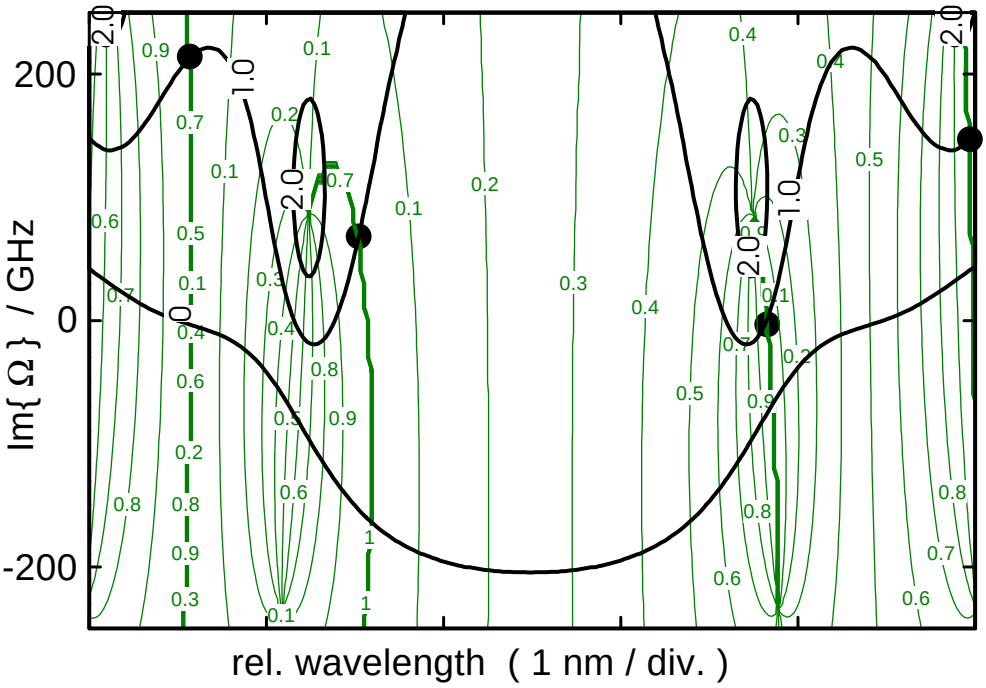

Fig. : Modes of the single section DFB laser in the $\Im m\,\Omega$-wavelength-plane. The left facet is antireflection coated. The right facet has a finite amplitude reflectivity r. The labels at the fat lines give the magnitude $d = -\ln(|r|)$ and the labels at the thin lines the phase $\varphi = \arg(r)$ of the reflectivity r.

Notice, that the two Figs. and are very similar. This is no occasion. In a single section DFB laser with spatially constant carrier density, the mode frequencies depend on carrier density according to

$$\Omega(N) = \Omega(N_{tr}) - \frac{1}{2}(\alpha_H + i)\; v_g \Gamma g'(N - N_{tr}). \qquad \text{single section laser only} \tag{6}$$

Thus, the lowest mode in the density-wavelength plot is always the lasing mode and there is no need to check it.

In multisection lasers, however, this may be different. We shall investigate this question when dealing with the lasers 1 and 2.

2.3 Local stability

Now we ask, whether a given stationary mode is stable against small perturbations.

For the answer, we use

$$2\gamma = \frac{1}{\tau} + \left(\frac{I}{e} - \frac{N}{\tau}\right)\; \partial_N\; \ln\left(g\Gamma_l\sqrt{K_z}\right), \tag{7}$$

$$\omega_r = \sqrt{\left(\frac{I}{e} - \frac{N}{\tau}\right)\partial_N(-2\Im m\,\Omega)} \tag{8}$$

for the small signal decay constant and resonance frequency, respectively, according to the single mode approach of Ref. [2]. The gain $g = g'\Gamma(N - N_{tr})$, the longitudinal fill factor Γ_l, and the longitudinal Petermann factor $\sqrt{K_z}$ can easily be calculated when integrating the CME for any given N, Ω. The partial derivative with respect to N has to be calculated for a constant right hand side of Equ. (3). This is a bit more complicated, because $\Omega(N)$ is only implicitely given. However, the rules of implicite differentiation yield

$$\left(\frac{\partial f}{\partial N}\right)_g = \left(\frac{\partial f}{\partial N}\right)_\Omega - \left(\frac{\partial g}{\partial N}\right)_\Omega \left(\frac{\partial f}{\partial \Omega}\right)_N \Big/ \left(\frac{\partial g}{\partial \Omega}\right)_N, \tag{9}$$

where $f(N, \Omega)$ denotes the quantity to be derived under the constriction that the left hand side of (3) is kept constant, $g(N, \Omega) = const.$

```
   1.57        zentr Wellenl in mikron
    1  1        Gainsection Anf Ende
    2  2        Phase Anf Ende
    3  3        reflector Anf Ende
  300    300    150    laengen in mikron
(180,0) (0,0) (180,0)  kappas in 1/cm
  -0.85    0     -3.20 stat det in nm
   25      20     25   optLoss cm^-1
  3.4     3.4     3.4  Gruppenindex
 (0.,0.)  (0.,0.)      AmpRfl left right
   0.9    diffGain 10^-16 cm^2
   -8     alfHenry
    1     Ntr 10^18cm^-3
    0.15  height AZ Mikron
    3     width  AZ Mikron
    3e8   Areko 1/s
   1e-10  Breko cm^3/s
   1e-28  Creko cm^6/s
     90   Strom Gainsektion (mA)
120  0  100 Stepzahl: Rebet Imbet N
 2.3 2.45   Anf Ende Wellenlaenge nm
  0 -0.02   Anf Ende ImOmega  10^12s^-1
 1.4  1.6   Anf Ende N        10^24m^-3
   0              lvar=Variante
```

Table 1: *Input parameter for the density-wavelength plot 'l1ellips' as well as for the combined Figs. 'l1fi'.*

```
   1.57        zentrale Wellenlaenge in mikron
    1  1        Gainsection Anf Ende
    2  2        Phase Anf Ende
    3  3        reflector Anf Ende
  300    300    150  laengen in mikron
(180,0) (0,0) (180,0)  kappas in 1/cm
  -0.85    0     -3.20     stat det nm
   25      20     25  optLoss cm^-1
  3.4     3.4     3.4  Gruppenindex
 (0.,0.)  (0.,0.)      AmpRef left  right
   0.9    diffGain 10^-16 cm^2
   -8    alfHenry
    1     Ntr 10^18cm^-3
    0.15  height AZ Mikron
    3     width  AZ Mikron
    3e8   Areko 1/s
   1e-10  Breko cm^3/s
   1e-28  Creko cm^6/s
     90   Strom Gainsektion (mA)
100 80 1  Stepzahl: Rebet Imbet N
 2.3 2.45 Anf Ende Wellenlaenge nm
-0.075   0.075 Anf Ende ImOmega  10^12s^-1
1.4  1.6       Anf Ende N        10^24m^-3
   0           lvar=Variante
```

Table 2: *Input parameter for the $\Im m\,\Omega$-wavelength plot in Fig. 'l1imom'. The step number 1 for N means that the Im-Re-Om-plot is done twice, one for 1.4, the second for 1.6.*

3 The Radziunas-device 1

3.1 Parameter

The input parameter used for the mode calculations are listed in the tables 1 and 2.

3.2 Spectral situation

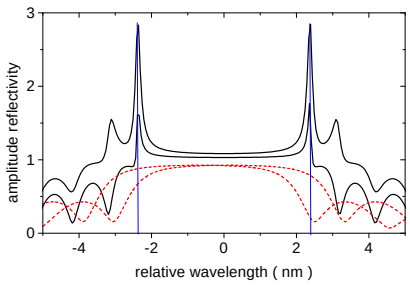

Fig. l1spec

The spectral situation for the density limits $N = 1.4$ and 1.6×10^{18} cm^{-3} are drawn in Fig. l1spec. Note that here as everywhere else in this paper the zero of the relative wavelength used as abscissa is the middle of the stop band of the laser section. Therefore, the spectra of the reflector shift, whereas the resonances ('ears') of the laser section spectra stay at the same position independent of N. This has the preference that only a fixed narrow range around these resonances needs to be considered in the following density-wavelength plots. For brevity, we will label the short wave resonance and its modes as 'negative' and the corresponding long wave side as 'positive', in the following. Between the two limiting densities, the negative 'ear' shifts across the falling slope of the reflectors stop band.

3.3 Stationary mode analysis versus time domain simulation

The left part of the $N\lambda$-plot in Fig. 'l1ellips' shows the stationary negative modes between -2.45 and -2.3 nm. The right part gives the same information for the positive modes between 2.3 and 2.45 nm relative wavelength. The fat and thin lines give the damping $d = \alpha_p L_p$ and the phase shift φ of the phase tuning section, respectively. The grey areas indicate the regions of local instability. The symbols are the results obtained by Radziunas with his time domain simulation for the case $d = 20\text{cm}^{-1} \times 300\mu\text{m} = 0.6$. They coincide very well with my curve for $d = 0.6$. The small differences for the negative modes can be attributed to the residual dispersion of the time domain model not contained in the stationary approach.

Observation 1a: Both approaches coincide with respect to wavelength and density.

Now we check the coincidence with respect to the phase. For these purposes, output power, carrier denstiy, as well as frequency and damping of power oscillations are drawn vs. the relative phase shift $\varphi/2\pi$ in Fig. 'l1fi'. The solid and dashed lines in these φ-plots are the data obtained by Radziunas from time domain simulations for decreasing and increasing the phase parameter stepwise from 1 to 0 and 0 to 1, respectively. Part a) shows the minimum and maximum power during a simulation interval. The + or - sign above the lines marks whether a negative or positive mode is lasing, respectively. The maximum and minimum powers are different between the points C and F for decreasing phase and between E and D for increasing phase. This indicates the appearence of well modulated self-pulsations. In the other regions, both lines coincide, indicating a stationary state. In the stationary regimes, the small signal frequency and damping constants have been obtained from the time domain model by analyzing the response to a small perturbation. In the SP regimes, f is the SP frequency determined from the power spectrum and the damping has been set to zero. The drawn time domain carrier density is the mean value over a SP period, in this case. The open circles and triangles in the parts b) to d) represent the statinary mode data for the negative and positive 'ears', respectively. Here, frequency and damping represent the small signal values in all cases.

As can be seen, the lines mostly follow one of the symbol tracks.

Observation 1b: Both approaches coincide also with respect to the phase.

Observation 2: The dynamical state of the laser can always be attributed to a certain mode.

The detailed discussion of both the $N\lambda$-plot and the φ-plot gives some further interesting information on the switching of SP by phase changes as well as on the mechanisms of mode jumps and on the background of the hystereses effects. This will be done step by step for the different intervalls indicated by the capital letters in part a) of the φ-plot. For compactness, we shall focus on the dominant modes, although several interesting nondominant modes can be observed.

A → B

Part a) of the φ-plot shows stationary lasing of a negative mode. In the lower parts of the figure, the black lines follow closely the triangles, which belong to the stationary mode with the lowest carrier density.

Observation 1c: Good agreement also for the small signal frequencies and damping constants. This holds for the stationary state of other intervals, too.

Observation 3a: The mode with the lowest carrier density is dominant in (A,B). This holds also for stationary states at other phases.

In the $N\lambda$-plot, this part of the dominant mode trace appears as the open sqares between the corresponding points A and B on the $d = 0.6$-ellipse.

B → C

Part a) of the φ-plotshows stationary emission of a positive mode. Again the solid lines follow the stationary mode with lowest density. The swiching of the dominant mode in point B from left to right 'ear' is obviously related to the densities of the stationary modes.

In the $N\lambda$-plot , the open circles between B and C correspond to this part of the phase change.

The damping of the dominant mode decreases in this interval and reaches zero at point C. At the same time, the frequency increases slightly.

C → F

Accordingly, point C is a Hopf bifurcation. The fingerprint of a corresponding transition to SP is clearly visible in the φ-plot.

The corresponding portion of the $N\lambda$-plot are the open circles between the points C and D. They scatter a bit because the wavelength is determined within the time domain simulation from the FFT of the output amplitude

with a limited frequency resolution. Note that they are completely located within the left grey instability area of the positive 'ear'.

The mean density during the SP fits surprisingly well to the density of the lowest stationary positive mode. Between C and E this is the absolutely lowest density. Between E and F, however, there are negative modes at considerably smaller densities. The self-pulsation stabilizes seemingly the positive lasing mode.

The frequency of the SP is smaller than the small signal resonance frequency. It keeps nearly constant within the whole SP range, whereas the latter one increases contineously.

In point F, the lasing switches from the self-pulsating positive mode into the stationary negative mode with the lowest density. Why does this happen just at this phase, not before and not thereafter? This cannot be explained neither by the φ-plot nor by the $N\lambda$-plot. The only pecularity of this point is that it seems to be the lowest point of the left 'ear' ellipses in the $N\lambda$-plot.

F → A

Stable operation of the lowest negative mode as already discussed for the interval A → B.

A → E

In point A we change the sign of the phase change and go back to larger values. The point F is passed in the lowest negative mode without noticeable reactions. This mode remains stable until point E. Again the small signal frequency and damping constants are well reproduced by the response to small perturbations in the time domain simulation. In the $N\lambda$-plot , this interval is represented by the black squares from F to E on the left side. They approach the border of the right grey area of instability just in point E.

This approach towards E is very interesting. Two modes meet in this point; one coming from the stable side, the other from the unstable side. These two modes cancel each other in point E. For phases larger than the E-value they disappear. The line of constant phase does no more intersect the line $d = 0.6$ in the $N\lambda$-plot. Accordingly, both f and γ go to zero when approaching point E.

What is this? A saddelnode bifurcation? Anyway, no Hopf bifurcation.

E → D

It must be shocking for the laser, when the phase is decreased through point E. Here the former dominant mode not only becomes unstable but disappears completely. The time domain simulation shows: the lasing switches to a self-pulsating negative mode. It is the negative mode with the lowest density in this range. There is still a positive mode with a distinctly smaller density, but again the self-pulsation seems to stabilize the higher-density mode.

In the $N\lambda$-plot , this SP of a negative mode appears at the very left as full squares between the labels E and D. This is close to but outside of the grey instability area. This seems to be a contradiction between the time domain simulation and the small signal stability analysis. However, such a behaviour can be expected when the border of the instablity region represents a subcritical Hopf bifurcation.

In point D the laser switches to the positive mode SP already described for the interval C → F. Again there is no apparant reason for the switching just in this point. It should be noted, however, that the position of this jump may also be an artefact of the finite simulation time.

D → C → B → A

Further increasing the phase, the laser follows the same states as observed for decreasing phase. Especially at point C, this behaviour is an indication that C represents a supercritical Hopf bifurcation.

Concluding this subsection:

1. Quantitative agreement between stationary mode analysis and time domain simulations for
   - phase tuning of stationary states
     (carrier density, small signal frequency and damping constants, switch betwee negative and positive modes)

- existence and position of a supercritical Hopf bifurcation into positive mode SP for decreasing phase

2. New observations / understanding by combining both approaches:
   - Stationary states seem always to be those modes with the lowest density.
   - The mean density of a self-pulsation agrees with the density of a stationary mode. This indicates the single mode type of SP and allows to identify which mode is self-pulsating.
   - The SP can prevent the transition into the mode with the lowest density.
   - The transition to a negative mode SP for increasing phase is connected with the disappearance of the dominant low-density negative mode. (Saddle node bifurcation ???)
3. open question: what determines the phase at which the SP cannot further stabilize a higher density mode (points F downphase and D upphase)?

References

[1] Mindaugas Radziunas, *Modelling of multi-section semiconductor DFB lasers. Part 1.*, report for the HHI, Oct. 29, 1999

[2] U. Bandelow, H.-J. Wünsche, and B. Sartorius, "Dispersive self Q-switching in DFB-lasers: theory versus experiment", IEEE Journal of Selected Topics in Quantum Electronics 3, pp. 270-278, 1997